

Journal of Geophysical Research: Atmospheres

RESEARCH ARTICLE

10.1029/2018JD029187

Key Points:

- iCAM5 can simulate the observed anticorrelation between stratiform rainfall fraction and precipitation oxygen isotope ratios
- All models can simulate the observed relationship between outgoing longwave radiation and precipitation oxygen isotope ratios
- The contribution of convective processes to precipitation oxygen isotope ratios is very site dependent

Supporting Information:

- Supporting Information S1

Correspondence to:

J. Hu,
hujun@usc.edu

Citation:

Hu J., Emile-Geay, J., Nusbaumer, J., & Noone, D. (2018). Impact of convective activity on precipitation $\delta^{18}\text{O}$ in isotope-enabled general circulation models. *Journal of Geophysical Research: Atmospheres*, 123, 13,595–13,610.
<https://doi.org/10.1029/2018JD029187>

Received 15 JUN 2018

Accepted 11 NOV 2018

Accepted article online 20 NOV 2018

Published online 10 DEC 2018

Impact of Convective Activity on Precipitation $\delta^{18}\text{O}$ in Isotope-Enabled General Circulation Models

Jun Hu¹ , Julien Emile-Geay¹ , Jesse Nusbaumer² , and David Noone³ 

¹Department of Earth Sciences, University of Southern California, Los Angeles, CA, USA, ²NASA Goddard Institute for Space Studies, New York, NY, USA, ³College of Earth, Ocean, and Atmospheric Sciences, Oregon State University, Corvallis, OR, USA

Abstract The $\delta^{18}\text{O}$ signal preserved in paleoarchives is widely used to reconstruct past climate conditions. In many speleothems, this signal is classically interpreted via the *amount effect*. However, recent work has shown that precipitation $\delta^{18}\text{O}$ ($\delta^{18}\text{O}_p$) is greatly influenced by convective processes distinct from precipitation amount, and new observations indicate that $\delta^{18}\text{O}_p$ is negatively correlated with the fraction of stratiform precipitation. Isotope-enabled climate models have emerged as a key interpretive tool in water isotope systematics, and it is thus important to determine to what extent they can reproduce these relationships. Here seven isotope-enabled models, including the state-of-the-art model iCAM5, are evaluated to see whether they can simulate the impact of convective activity on $\delta^{18}\text{O}_p$ in observations. The results show that, of these models, only iCAM5 can simulate the observed anticorrelation between stratiform fraction and $\delta^{18}\text{O}_p$. Furthermore, while all models can simulate the observed relationship between outgoing longwave radiation and $\delta^{18}\text{O}_p$, different models achieve this via different mechanisms—some getting the right answer for the wrong reasons. Because iCAM5 appears in various metrics to correctly simulate $\delta^{18}\text{O}_p$ variability, we use it to examine long-standing interpretations of $\delta^{18}\text{O}_p$ over Asia. We find that the contribution of convective processes is very site dependent, with local processes accounting for a very small amount of variance at the sites of most Chinese cave records (speleothems). The residual is attributed to source and transport effects. Our results imply that state-of-the-art models like iCAM5 can and should be used to guide the interpretation of $\delta^{18}\text{O}_p$ -based proxies.

1. Introduction

The $\delta^{18}\text{O}$ signal preserved in paleoarchives (e.g., corals, speleothem, tree ring cellulose, and ice cores) is widely used to reconstruct past climate conditions. In the tropics, the inverse relationship between precipitation $\delta^{18}\text{O}$ and precipitation amount, namely, the *amount effect* (Dansgaard, 1964), is often invoked to interpret $\delta^{18}\text{O}$ as a proxy for precipitation amount (Cheng et al., 2006; Yadava et al., 2004; Yuan et al., 2004). However, recent studies have shown that precipitation $\delta^{18}\text{O}$ ($\delta^{18}\text{O}_p$) is controlled by a wider range of processes.

Observational studies of $\delta^{18}\text{O}_p$ reveal that convective storms, especially organized convective systems, generate lower $\delta^{18}\text{O}_p$ than nonconvective storms or disorganized convection (Kurita, 2013; Kurita et al., 2011; Lawrence et al., 2004; Lekshmy et al., 2014; Moerman et al., 2013; Risi et al., 2008) and suggest that $\delta^{18}\text{O}_p$ can reflect intraseasonal variability like the Madden-Julian Oscillation (Kurita et al., 2011) or tropical cyclone activity (Frappier et al., 2007). The mechanisms are still debated. The recycling of low $\delta^{18}\text{O}$ water vapor below the cloud base in convective systems may contribute to the decrease of $\delta^{18}\text{O}_p$ (Risi et al., 2008), and raindrop reevaporation depletes the surrounding water vapor (Lee & Fung, 2008). Convection depth and condensation height are other important factors. Lacour et al. (2018) find that deep convection is associated with isotopically depleted water vapor and precipitation, while Cai and Tian (2016) show that the cloud-top height correlates well with $\delta^{18}\text{O}_p$.

A recent observational study (Aggarwal et al., 2016) revealed a negative correlation between stratiform fraction (ratio of stratiform precipitation to total precipitation) and $\delta^{18}\text{O}_p$, providing a new yardstick for model evaluation ($R^2 = 0.59$, p value < 0.0001). They used Tropical Rainfall Measuring Mission (TRMM) 2A25/2A23 satellite data ($2.5^\circ \times 2.5^\circ$) and $\delta^{18}\text{O}_p$ at GNIP stations from 1998 to 2014 and compared the stratiform rainfall fraction to the $\delta^{18}\text{O}_p$ data (Figure 1). They proposed that convective precipitation was generated from strong

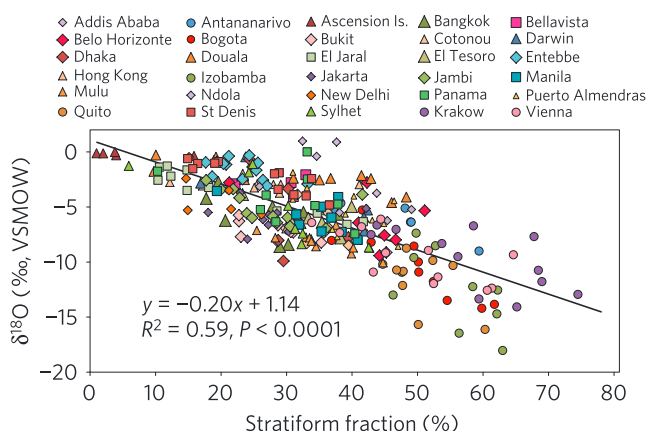


Figure 1. Correlation of mean monthly $\delta^{18}\text{O}$ (GNIP station data) and stratiform fraction (Tropical Rainfall Measuring Mission satellite data). From Aggarwal et al. (2016, Figure 1).

are very common in the tropics, accounting for about 50% of tropical precipitation (Nesbitt et al., 2006), and feature both convective and large stratiform regions. Thus, when stratiform precipitation comes to dominate in MCSs, these organized convective systems may generate $\delta^{18}\text{O}$ -depleted precipitation.

Isotope-enabled models are useful tools to study the variability of $\delta^{18}\text{O}_p$ by separating different factors influencing $\delta^{18}\text{O}_p$ (Hoffmann et al., 1998; Joussaume et al., 1984; Jouzel et al., 1987; Noone & Simmonds, 2002; Schmidt et al., 2007; Yoshimura et al., 2008), and since they can fill in the gaps between climate variables and paleoclimate records with the aid of proxy system models (Dee, Emile-Geay, et al., 2015; Evans et al., 2013), they can be directly exploited to investigate the variability of paleoclimate proxies (Baker et al., 2012; Dee et al., 2017; Jex et al., 2013). Since convective activity plays an important role, it is important to determine to what extent isotope-enabled climate models can reproduce the relationships between convection and $\delta^{18}\text{O}_p$. This evaluation will give insights into possible improvements in current isotope-enabled models. If models can grasp the convection- $\delta^{18}\text{O}_p$ relationship, it will help justify their use in investigating the variability of $\delta^{18}\text{O}_p$ and interpret paleoclimate records based on it.

Another reason for probing this relationship is that stable water isotopes provide unique constraints on general circulation model (GCM) performance. They offer opportunities to constrain physical processes such as cloud and convection schemes in GCMs by comparing with traditional observations (including instrumental observations from ground stations, satellites, and aircraft). For instance, previous studies have probed the sensitivity to parameters in convection schemes, such as the time scale for consumption of convective available potential energy (Lee et al., 2009; Tharammal et al., 2017), convective available potential energy thresholds (Nusbaumer et al., 2017), entrainment rate (Field et al., 2014), and others (Bony et al., 2008; Risi et al., 2012). In this paper, we use the observed relationship between convection types/depth and $\delta^{18}\text{O}_p$ as another yardstick to constrain convective processes in GCMs.

As an application, we explore how the quantification of these relationships affects the interpretation of paleohydrological records based on $\delta^{18}\text{O}_p$, particularly $\delta^{18}\text{O}$ from Asian speleothems. Traditionally, the $\delta^{18}\text{O}$ of Asian speleothem calcite has been interpreted as an indicator of (a) regional precipitation, (b) the ratio of summer to winter precipitation, or (c) monsoon intensity (Cheng et al., 2009; Dykoski et al., 2005; Wang et al., 2001, 2008). This assumes that the amount effect is dominant, though recent studies have shown that Asian speleothem $\delta^{18}\text{O}$ can also be determined by upstream water vapor $\delta^{18}\text{O}$ (Pausata et al., 2011), the variability of moisture sources (Tian et al., 2007), changes in atmospheric circulation (Maher & Thompson, 2012; Tan, 2014), and convective activity (Cai & Tian, 2016; Kurita, 2013; Lekshmy et al., 2014). Thus, it is necessary to compare the relative contributions impacting $\delta^{18}\text{O}_p$, which will help constrain the interpretation of these records. This is of great importance because Asian monsoon systems ultimately provide water supporting over 4 billion people, and speleothem records provide a unique window into the natural variability of these systems.

The paper is structured as follows: we introduce data and methods in section 2 and evaluate how isotope-enabled models simulate the relationship between convective activity and $\delta^{18}\text{O}_p$ in section 3. Section 4 discusses the implications of the evaluation results and provides our conclusions.

updrafts, which brings isotopically enriched water vapor up, making $\delta^{18}\text{O}_p$ higher. For the stratiform precipitation, raindrops formed from the $\delta^{18}\text{O}$ -depleted water vapor in the midtroposphere, resulting in more negative $\delta^{18}\text{O}_p$.

Aggarwal et al.'s (2016) conclusion that more stratiform rainfall fraction is associated with lower $\delta^{18}\text{O}_p$ does not conflict with previous findings that organized convection corresponds to low $\delta^{18}\text{O}_p$. In the tropics, organized convection is associated with a higher stratiform fraction. Stratiform precipitation is often thought to occur only in fronts and cyclones in the midlatitudes, but it can also occur in the tropics and even account for a large portion of the tropical rainfall, especially in mesoscale convective systems (MCSs). In the tropics, precipitation is often the product of young/vigorous convection (with strong vertical air motion), which generates *convective* precipitation, or old/less active convection (with weaker vertical air motion), which generates *stratiform* precipitation and shares similar characteristics to midlatitude stratiform precipitation (Houze, 1997). For example, MCSs constitute organized convection. They

Table 1
General Circulation Models Used in this study

Model	Resolutions	Nudging	Time periods	Convection schemes	Reference
LMDZ ^a	2.5° × 3.75°	Yes	1979–2007	Emanuel and Živković-Rothman (1999)	Risi et al. (2010)
CAM2 ^a	2.81° × 2.81°	No	1974–2003	Zhang and McFarlane (1995)	Lee et al. (2007)
isoGSM ^a	1.9° × 1.875°	Yes	1979–2009	Moorthi and Suarez (1992)	Yoshimura et al. (2008)
MIROC ^a	2.8° × 2.8°	No	1979–2007	Arakawa and Schubert (1974)	Kurita et al. (2011)
HadAM4 ^a	2.5° × 3.75°	No	1972–2001	Gregory and Rowntree (1990)	Tindall et al. (2009)
SPEEDY-IER	3.75° × 3.75°	No	1966–2000	simplified: Tiedtke (1989)	Dee, Noone, et al. (2015)
iCAM5	0.9° × 1.25°	No	1971–2005	deep convection: Zhang and McFarlane (1995) shallow convection: Park and Bretherton (2009)	Nusbaumer et al. (2017)

^aA SWING2 model.

2. Data and Methods

The model outputs analyzed here are from LMDZ, CAM2, isoGSM, MIROC, and HadAM4 as part of the Stable Water Isotope Intercomparison Group, Phase 2 (SWING2) project (Risi et al., 2012; <https://data.giss.nasa.gov/swing2/>), forced by observed sea surface temperature (SST) and sea ice following the Atmospheric Model Intercomparison Project protocol (Hurrell et al., 2008). The results of SPEEDY-IER and iCAM5 are also from an Atmospheric Model Intercomparison Project-style experiment (see Table 1 for references). Here we call the models participating in the SWING2 project *SWING2 models*. iCAM5 is a state-of-the-art isotope-enabled models, with finer resolution, complex convection, and stratiform cloud physics schemes, including the conversions of cloud water species (liquid, ice, vapor, and snow) and subgrid-scale processes in clouds (Nusbaumer et al., 2017). In the rest of this paper, convective rainfall will be identified with the models's *convective precipitation* variable (CONV) and stratiform precipitation with the *large-scale* (LS) precipitation variable. The impacts of this approximation are discussed below.

TRMM 3A25 (monthly data with the resolution of 1° × 1°, 1998–2014) is used to calculate the observed climatological stratiform rainfall fraction in the tropics. In TRMM 3A25, the rainfall type in one pixel is identified by comparing its reflectivity to the averaged nearby reflectivity. If the reflectivity of a pixel exceeds the surrounding background by a factor f , the pixel is considered to be convective. The f is a function of the background reflectivity intensity and is calibrated to match a manual separation of convective/stratiform regions where a bright band is identified in radar echoes. A bright band is a sufficient condition for a region to be stratiform. A detailed description of this algorithm can be found in http://www.eorc.jaxa.jp/TRMM/documents/PR_algorithm_product_information/pr_manual/PR_Instruction_Manual_V7_L1.pdf.

GCMs commonly generate convective precipitation within their convection schemes and produce LS precipitation within their cloud/microphysics schemes. In GCMs, the convection process consumes water vapor, forming convective precipitation, with vertical air motion and adjustments of temperature and humidity profiles. Then, cloud/microphysics schemes produce LS precipitation from the remaining water vapor if a saturation condition is reached. By definition, all precipitation formed as part of this convection process is convective (CONV) precipitation. In nature, convective and stratiform precipitation occur simultaneously, and stratiform precipitation may account for a large fraction of precipitation in convection. TRMM observational analyses use satellite-based radar reflectivity to distinguish convective and stratiform precipitation because the difference in radar reflectivity characteristics can ensure that the classified precipitation has the characteristics described in Houze (1997). Therefore, although the separation scheme of convective and stratiform precipitation in TRMM is different from that in models, they intend to partition both convective and stratiform precipitation as in Houze (1997): Young/vigorous convection with strong vertical motion is categorized as convective precipitation, while old/inactive convection with weak vertical motion is categorized as stratiform precipitation. Also, TRMM satellite data were used to evaluate convective and stratiform precipitation in climate models in previous studies (Dai, 2006; Song & Yu, 2004). Thus, in this paper the simulation of convective/stratiform precipitation in GCMs is compared with TRMM observations and the results of Aggarwal et al. (2016). The *stratiform fraction* in model simulations is calculated as the ratio of LS precipitation to total precipitation (CONV + LS).

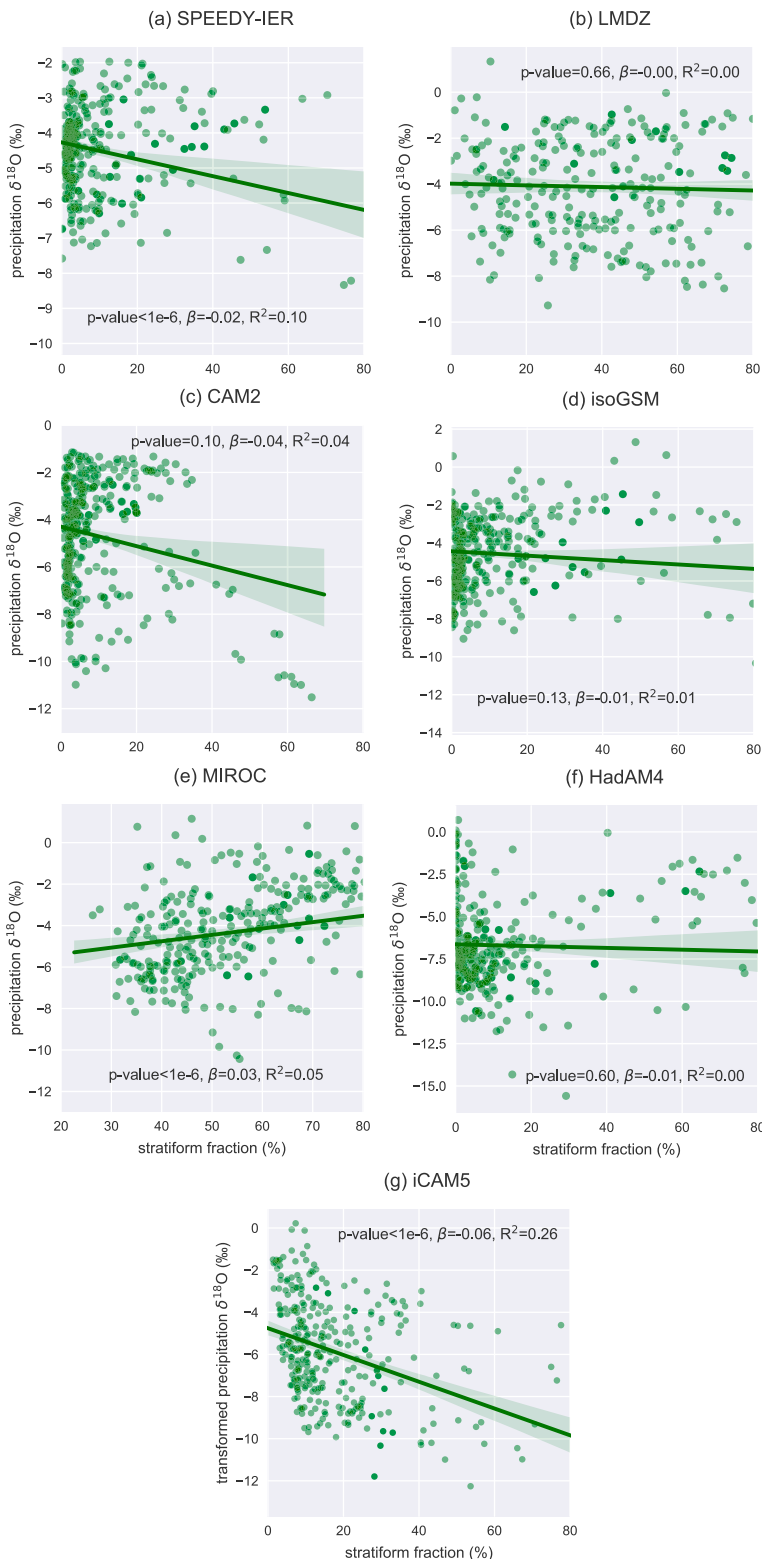


Figure 2. Relationship between monthly stratiform precipitation fraction and $\delta^{18}\text{O}_P$ at the same locations as Aggarwal et al. (2016) in (a) SPEEDY-IER, (b) LMDZ, (c) CAM2, (d) isoGSM, (e) MIROC, (f) HadAM4, and (g) iCAM5. The β values are ordinary least square slopes.

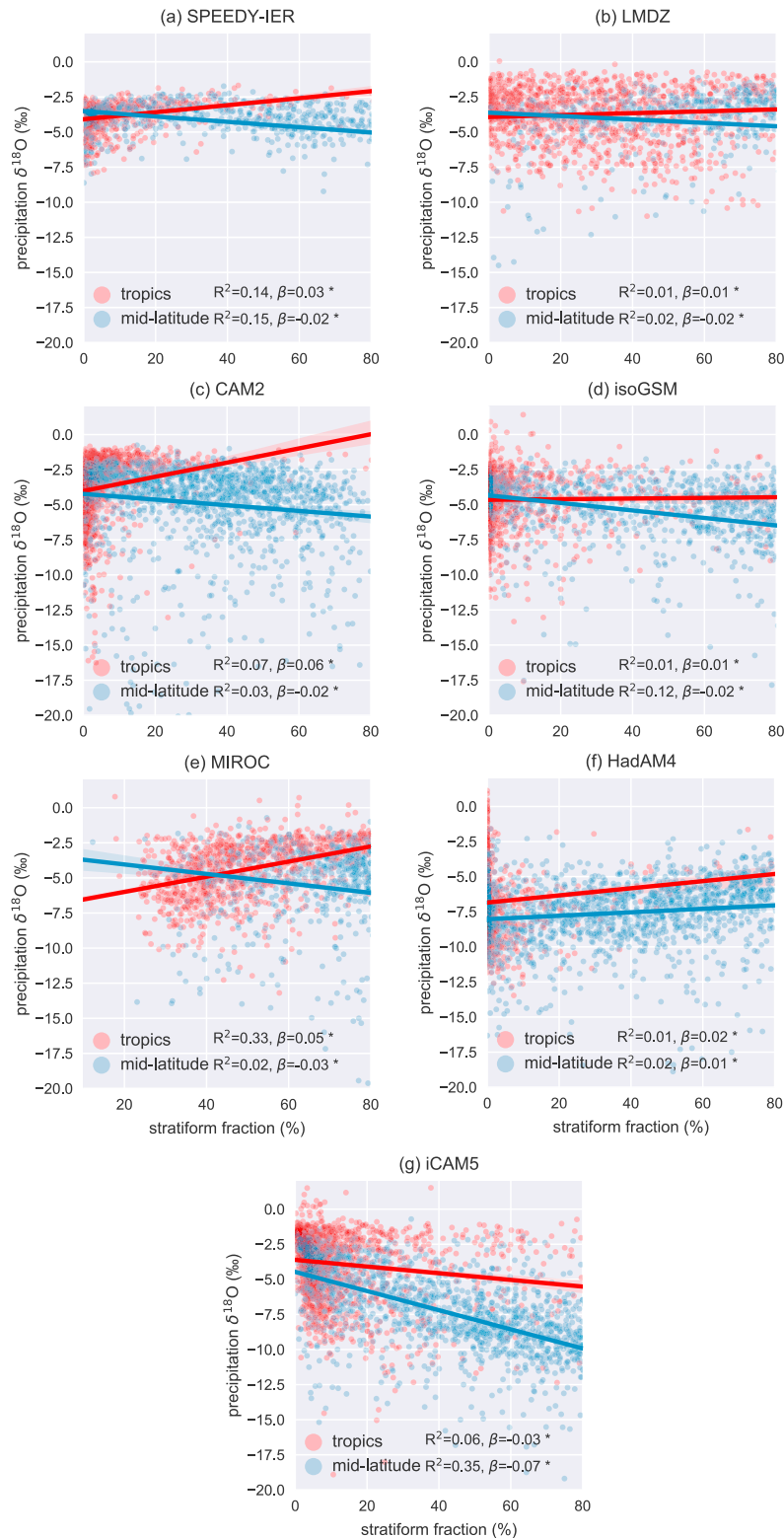


Figure 3. Relationship between monthly stratiform precipitation fraction and $\delta^{18}\text{O}_P$ in the tropics and midlatitudes in (a) SPEEDY-IER, (b) LMDZ, (c) CAM2, (d) isoGSM, (e) MIROC, (f) HadAM4, and (g) iCAM5. The β values are ordinary least square slopes. Stars behind β values represent the correlation passing the 95% level with an isospectral test.

All correlations calculated in the paper are based on monthly data. When establishing significance, we use an isospectral test (Ebisuzaki, 1997) to control for autocorrelation, and we use the false discovery rate method (Benjamini & Hochberg, 1995) to control for the multiple hypothesis test problem. See Hu et al. (2017) for why it is essential to control for both effects.

3. Results

3.1. Correlation Between Stratiform Precipitation Fraction and $\delta^{18}\text{O}_p$

Here we evaluate whether isotope-enabled models can simulate the negative correlation between stratiform rainfall fraction and $\delta^{18}\text{O}_p$. Figure 2 shows the relationship between stratiform fraction and $\delta^{18}\text{O}_p$ in our seven models, over the grid boxes colocated with the GNIP stations analyzed in Aggarwal et al. (2016). SPEEDY-IER, CAM2, isOGSM, and iCAM5 appear to simulate the observed anticorrelation, albeit with relatively low R^2 values; iCAM5 has the largest such value but still underestimates the slope. Since the distribution of stratiform fraction is nonnormal, we also transform it to normality (Emile-Geay & Tingley, 2016; Figures S1 and S2 in the supporting information) and the results are the same.

To see how models simulate this relationship at other locations, Figure 3 collects grid boxes in the tropics (red dots, 30°S to 30°N) and midlatitudes (blue dots, 50–30°S and 30–50°N) and displays the relationship between stratiform fraction and $\delta^{18}\text{O}_p$ (results of transformed stratiform fraction is shown in Figures S3 and S4). All models except HadAM4 simulate negative correlations in the midlatitudes, but in the tropics, all models except iCAM5 simulate positive correlations, which is inconsistent with observations (Aggarwal et al., 2016). Only iCAM5 simulates the negative correlation, though with an R^2 value smaller than observed. Considering the uncertainties from both the observations and models, we focus mainly on a qualitative comparison, looking at the sign of correlation, not the magnitude. Even by this permissive criterion, only iCAM5 successfully simulates the observed negative correlation between stratiform fraction and $\delta^{18}\text{O}_p$ in the tropics.

To see this another way, Figure 4 shows the spatial distribution of the correlation between stratiform fraction and $\delta^{18}\text{O}_p$ over the globe (correlations between monthly time series of stratiform fraction and $\delta^{18}\text{O}_p$ at each grid cell). All models simulate negative correlations in the continental midlatitudes, but all models except iCAM5 simulate positive correlations in the tropics. iCAM5 is the only model to simulate negative correlations over most areas in both tropics and midlatitudes, as in observations. LMDZ simulates the negative correlations only over the Indo-Pacific warm pool in the tropics. In the continental midlatitudes, cold seasons tend to see larger stratiform fractions (smaller convective fractions) and cold temperatures, leading to lower $\delta^{18}\text{O}_p$. All models except iCAM5 simulate positive correlations over the midlatitude oceans. This cannot be constrained by GNIP observations since stations are all on land. One possible explanation for this is that midlatitude cyclones bring in warmer and more isotopically enriched air, while at the same time generating large stratiform precipitation fractions, producing the positive correlations. All models can simulate both relationships, so all models generate negative correlations between stratiform fraction and $\delta^{18}\text{O}_p$ there. In the tropics, seasonal variability is small, so the correlation between stratiform fraction and $\delta^{18}\text{O}_p$ is more dependent on convection and microphysics schemes (it is a more sensitive indicator of model verisimilitude for these processes, and it appears that no particular type of convection scheme improves simulating this relationship). Some oceanic regions immediately west of continents show positive correlations in iCAM5. These are arid regions where climatological monthly precipitation is less than 1.5 mm/day (masked regions in Figure 9), so the uncertainty of stratiform precipitation fraction is high. Many of these regions are also places where stratiform clouds always exist, so the separation between convective and stratiform precipitation is somewhat arbitrary since stratiform clouds always present. Whether the results of Aggarwal et al. (2016) apply for these regions needs future investigation.

It should be noted that the observations themselves are affected by their own uncertainties. For example, the stratiform fraction in Aggarwal et al. (2016) is retrieved from satellite-based reflectivity. There are uncertainties in the satellite observation itself and the conversion process. Also, the estimated stratiform fraction hinges on the criteria for the classification of stratiform and convective precipitation (e.g., including shallow nonisolated precipitation in stratiform precipitation or not; Funk et al., 2013). Finally, the relationship revealed in Aggarwal et al. (2016) is based on a relatively short time series (monthly data for 16 years vs. 29 to 35 years for GCMs).

To better understand why iCAM5 can simulate the negative relationship between stratiform fraction and $\delta^{18}\text{O}_p$, its cloud microphysical processes over tropical convective and stratiform regions are diagnosed in Figure 5. The water vapor $\delta^{18}\text{O}$ vertical profile shows more depleted vapor over stratiform than convective

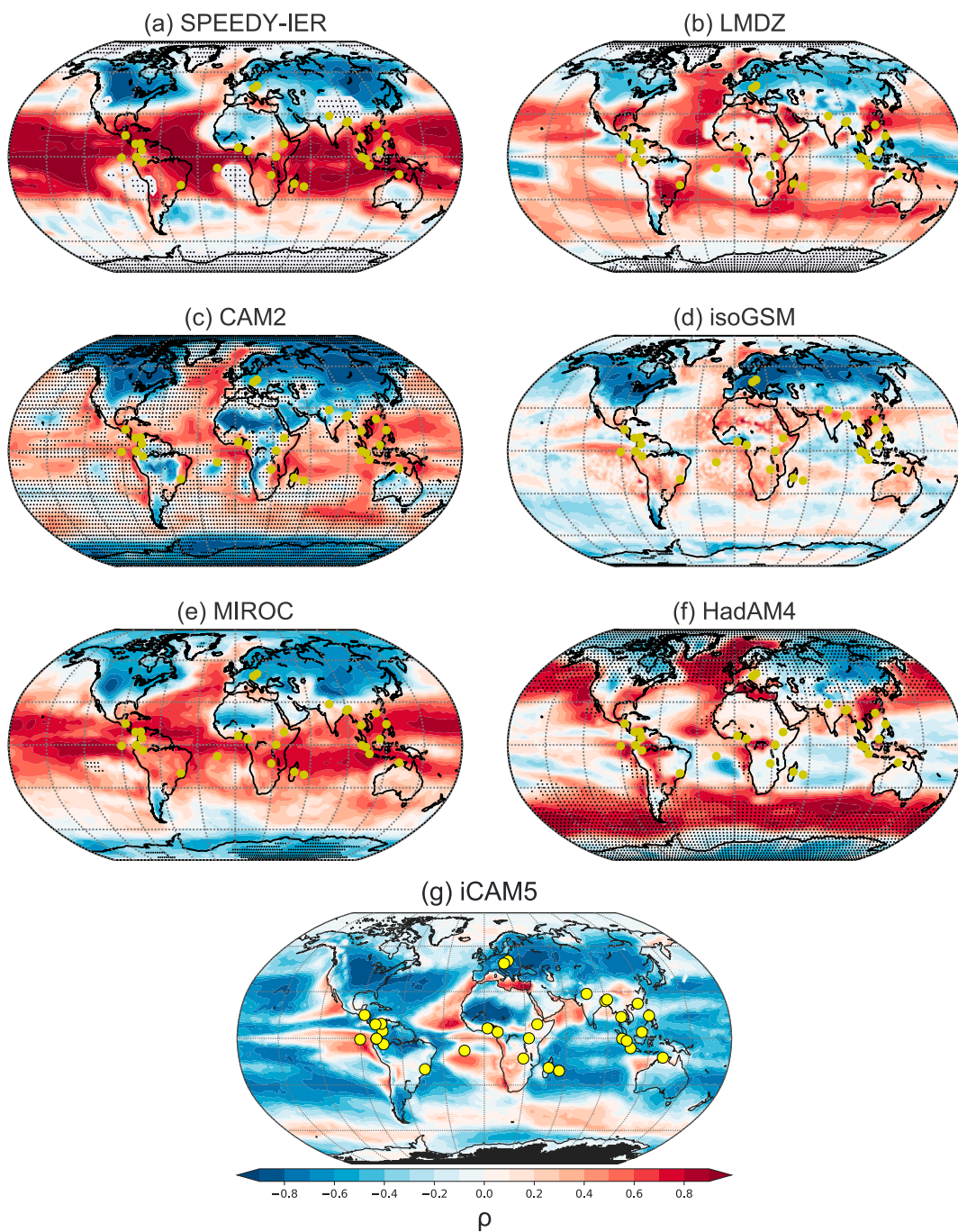


Figure 4. Correlation between monthly stratiform precipitation fraction and $\delta^{18}\text{O}_p$ in (a–g) seven models. Dots represent correlation not passing the 95% level significance isospectral test. Yellow circles mark the locations of GNIP stations analyzed in Aggarwal et al. (2016).

regions, and more ^{18}O -depleted water vapor will form more negative $\delta^{18}\text{O}_p$. The deuterium excess of water vapor (d) can be an indicator of kinetic effects, which occur during vapor deposition onto ice particles and reevaporation of rain in low humidity environments (Kurita et al., 2011). Figure 5b shows that iCAM5 simulates higher d values in the middle to upper troposphere (600–300 hPa) in stratiform regions than convective regions. This indicates that more ice crystals form in the upper troposphere over stratiform regions. The condensation heating profile (Figure 5c) also confirms that stratiform regions have more condensation in the upper levels than convective regions. Since more ice particles are generated from ^{18}O -depleted water vapor,

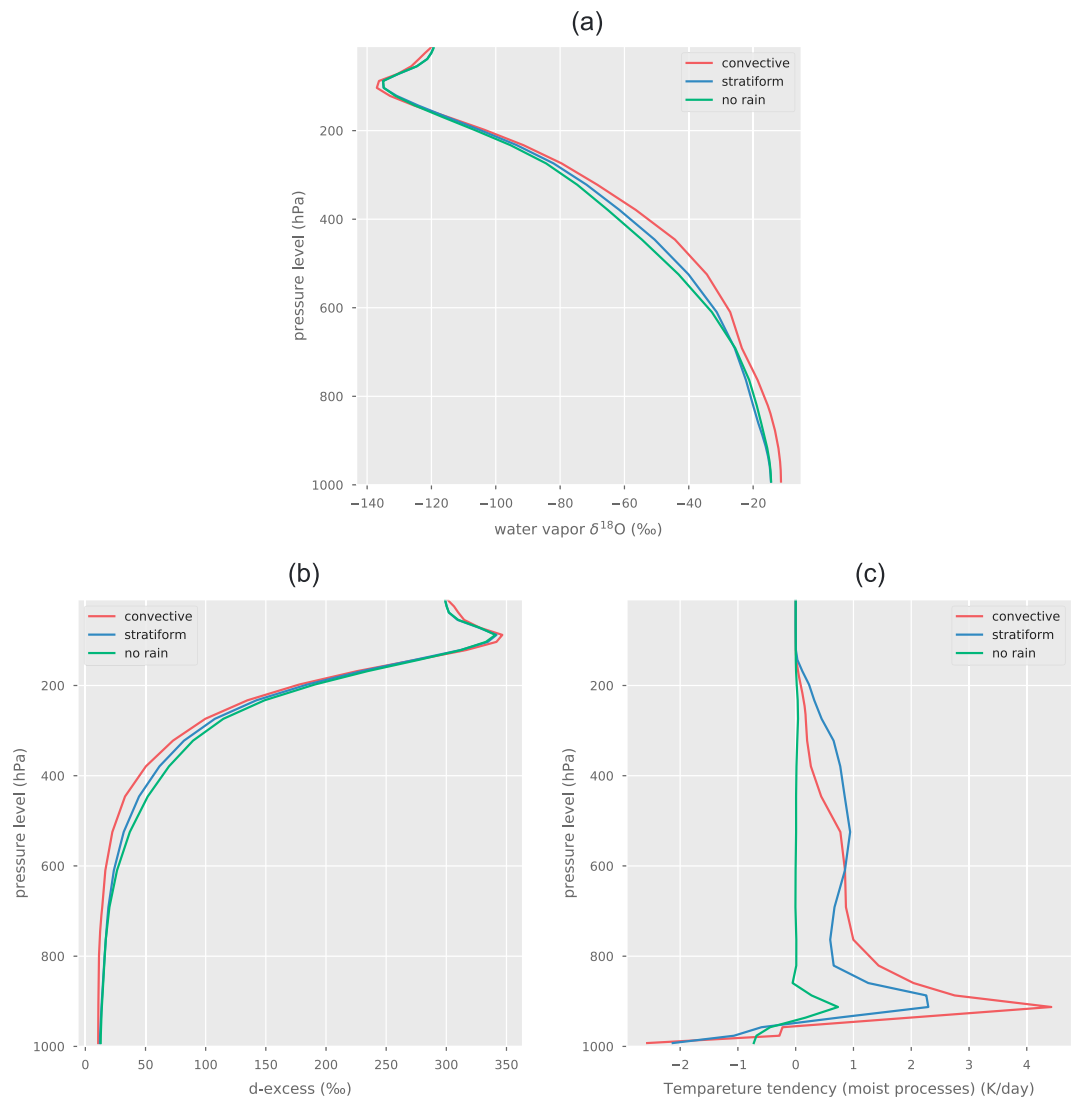


Figure 5. Vertical profiles of (a) water vapor $\delta^{18}\text{O}$, (b) deuterium excess, and (c) condensational heating over the convective rainfall region, the stratiform rainfall region, and no rain region in the tropics (30°S to 30°N) in iCAM5. The convective/stratiform rainfall region is where the proportion of convective/stratiform rainfall to total rainfall exceeds 0.8.

these particles have a more negative $\delta^{18}\text{O}$ when they precipitate to the ground, resulting in lower $\delta^{18}\text{O}_p$. This process is consistent with Aggarwal et al. (2016) in that stratiform precipitation mainly forms with the ^{18}O -depleted water vapor in the upper atmosphere. Another possible explanation for the high d values in the upper troposphere over stratiform regions in iCAM5 is that stratiform precipitation is fed by water vapor, which has been recycled via the reevaporation of rain, following the moisture recycling processes revealed in Risi et al. (2008) and Kurita et al. (2011). This is consistent with the iCAM5 code, in which the LS cloud physics always triggers after the convection. The vertical profiles of deuterium excess of water vapor in other models (Figure S6) show that only LMDZ simulates higher d values in the middle to upper troposphere (600–300 hPa) over stratiform regions like iCAM5, but its d values decrease with altitude from surface to 400 hPa.

Therefore, the reason iCAM5 can simulate the observed negative correlation between stratiform ratio and $\delta^{18}\text{O}_p$ can be directly tied to its more faithful representation of the vertical distribution of cloud condensate. This gives us confidence in using this model to study the role of convection in the interpretation of $\delta^{18}\text{O}_p$ and paleohydrological records (section 3.3). Also, this indicates that $\delta^{18}\text{O}_p$ is a sensitive indicator of the stratiform cloud environment and can therefore help inform the model development cycle.

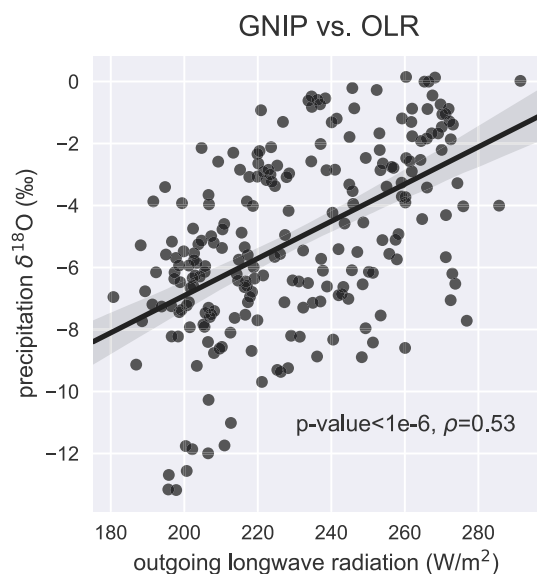


Figure 6. Relationship between National Oceanic and Atmospheric Administration interpolated outgoing longwave radiation (OLR) and GNIP $\delta^{18}\text{O}_p$ over the stations in Aggarwal et al. (2016), excluding stations higher than 2,000 m (four stations).

3.2. Correlation Between Outgoing Longwave Radiation and $\delta^{18}\text{O}_p$

Here we use outgoing longwave radiation (OLR) to track LS convective activity. Vigorous convection is usually deep, so the cloud-top temperature is cold, emitting lower OLR than weak/shallow convection. Since strong convection corresponds to low $\delta^{18}\text{O}_p$, OLR displays a positive correlation with $\delta^{18}\text{O}_p$ in observations (Lekshmy et al., 2014; Moerman et al., 2013). National Oceanic and Atmospheric Administration interpolated OLR (Liebmann, 1996) and GNIP $\delta^{18}\text{O}_p$ over the stations in Aggarwal et al. (2016) also display this positive relationship (Figure 6). Here we exclude four stations above 2,000 m since the OLR data set cannot capture the topography of the tropical Andes due to its low spatial resolution, thus may not be representative of the local climate conditions observed by those stations. OLR is also a direct indicator of convection depth, so it can be used to examine whether models can simulate the relationship between convection depth and $\delta^{18}\text{O}_p$. Deep convection (low OLR) is associated with low $\delta^{18}\text{O}_p$ in the observations (Lacour et al., 2018), so OLR also should bear a positive correlation to $\delta^{18}\text{O}_p$. In the midlatitudes, where convection is much less than the tropics, OLR is more dependent on surface temperature. In summer, surface temperature is higher, leading to higher OLR, and $\delta^{18}\text{O}_p$ also usually reaches its peak due to the temperature effect (Dansgaard, 1964; Galewsky et al., 2016) and vice versa for winter. This makes the variation of OLR and $\delta^{18}\text{O}_p$ in phase in the midlatitudes.

Since only four out of seven models (SPEEDY-IER, LMDZ, isoGSM, and iCAM5) provide the OLR variable, we restrict the analysis to these four models. All four models (Figure 7) simulate the positive correlations between

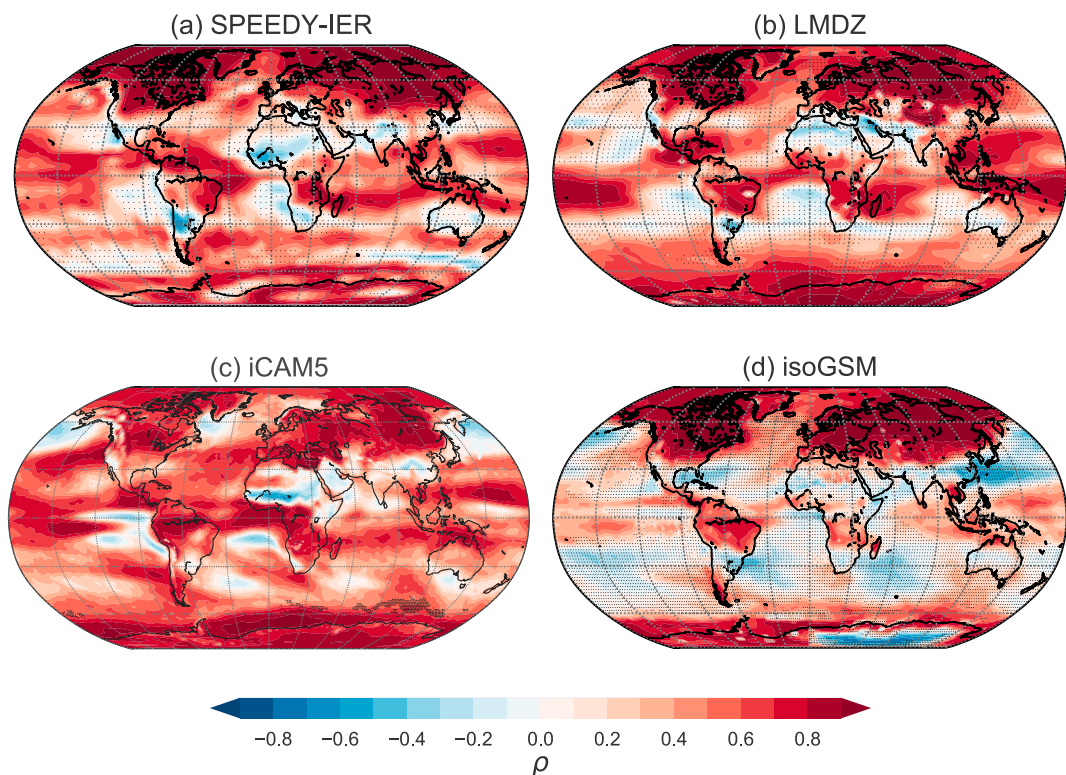


Figure 7. Correlation between monthly outgoing longwave radiation and $\delta^{18}\text{O}_p$ in (a–d) four models. Dots represent correlation not passing the 95% level significance isospectral test.

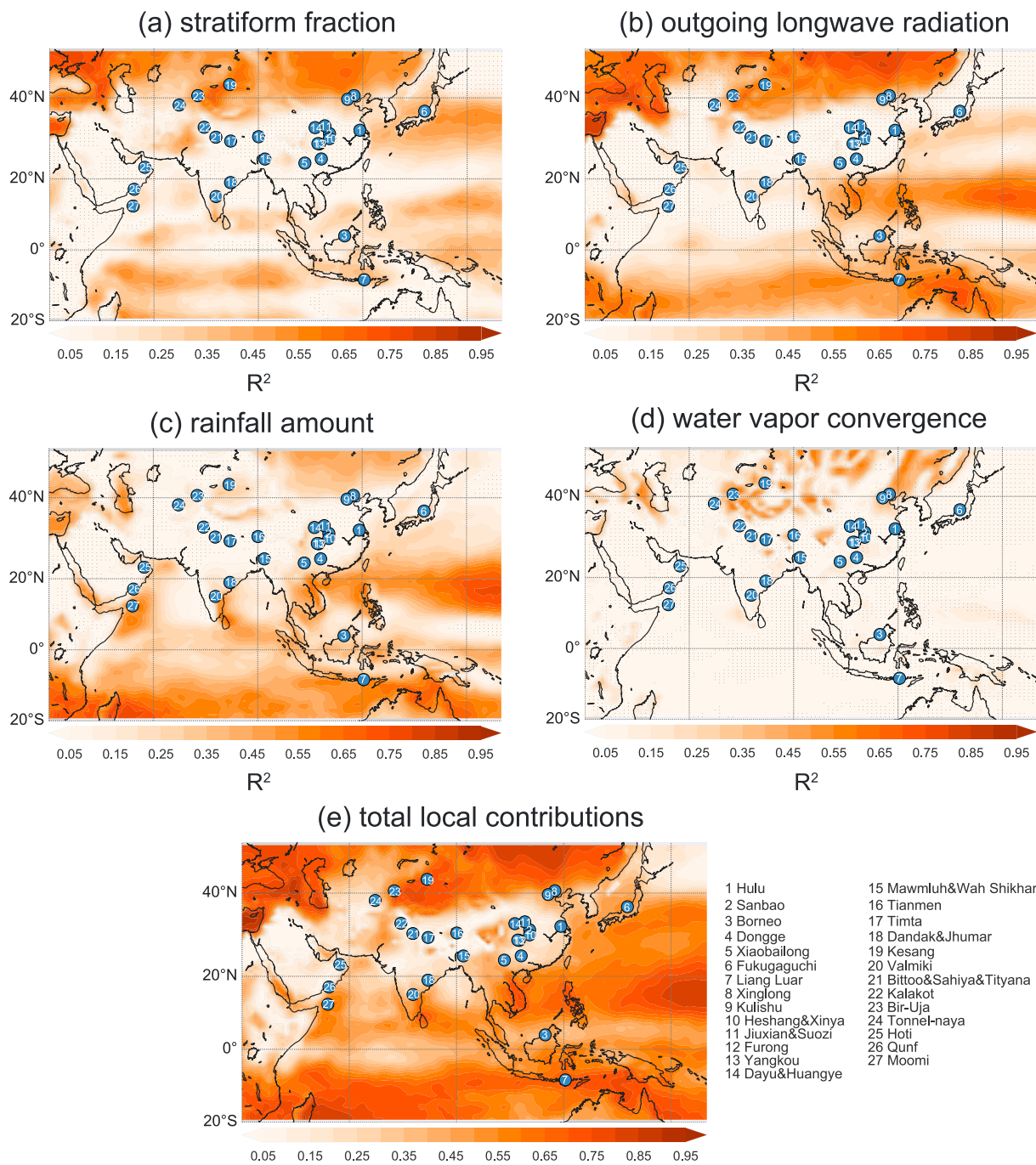


Figure 8. The variance of monthly $\delta^{18}\text{O}_p$ explained by (a) stratiform rainfall fraction, (b) outgoing longwave radiation, (c) precipitation amount, (d) local water vapor convergence, and (e) the total local contributions in iCAM5. Blue dots are cave sites collected in the global speleothem database SISAL_v1, and the names of these caves are listed beside Figure 8e.

OLR and $\delta^{18}\text{O}_p$ in both tropics and midlatitudes, consistent with the observations. Nonetheless, different models achieve this relationship through different mechanisms. iCAM5, which successfully reproduces the negative correlation between $\delta^{18}\text{O}_p$ and stratiform fraction, can simulate this relationship because its strong LS convective regions (low OLR) are associated with more stratiform precipitation, generating lower $\delta^{18}\text{O}_p$. On the other hand, models like SPEEDY-IER, LMDZ, and isoGSM, which do not reproduce the anticorrelation between $\delta^{18}\text{O}_p$ and stratiform fraction, simulate this relationship because stronger convection generates more precipitation, so rainout processes produce lower $\delta^{18}\text{O}_p$. This is not related to the discrimination of

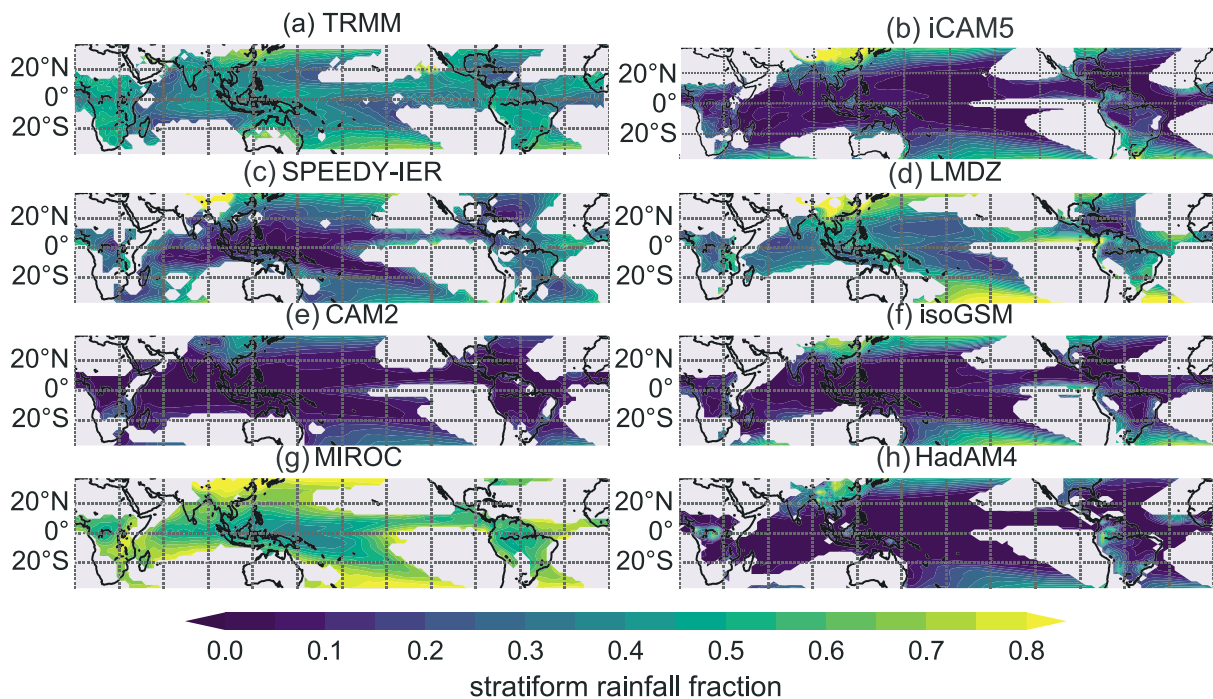


Figure 9. Climatological stratiform fraction in the tropics from (a) satellite observations and (b–h) isotope-enabled models. Regions where climatological precipitation is less than 1.5 mm/day are masked.

isotope modules in convection and nonconvection processes, so the $\delta^{18}\text{O}_p$ -OLR link is a less sensitive metric of model performance.

From the viewpoint of convection depth, the fact that all models simulate the positive correlations between OLR and $\delta^{18}\text{O}_p$ indirectly shows that models can correctly simulate the relationship between convection depth and $\delta^{18}\text{O}_p$ (Lacour et al., 2018). The direct examination of how models simulate this relationship is currently limited by the accessibility of the condensation heating variable in SWING2 models.

In summary, all models simulate the observed positive correlation between OLR and $\delta^{18}\text{O}_p$ in the tropics and midlatitudes. Since OLR is an indicator of the intensity of LS convection and convection depth, this result suggests that current isotope-enabled models can be used to study the role of convection depth or LS convection intensity in $\delta^{18}\text{O}_p$ and paleoclimate proxies.

3.3. Implications for Speleothem Record Interpretation

As mentioned before, the $\delta^{18}\text{O}$ of speleothem calcite is frequently used as an indicator of past hydrological conditions (Cheng et al., 2016; Sinha et al., 2011). Since cave $\delta^{18}\text{O}$ is driven by variations in $\delta^{18}\text{O}_p$, understanding the latter is critical to interpreting these records, and $\delta^{18}\text{O}_p$ is controlled by multiple factors including convective activity, rather than an indicator of regional precipitation or monsoon intensity. Thus, it is necessary to compare the relative contributions of different factors impacting $\delta^{18}\text{O}_p$, which will help constrain the interpretation of speleothem $\delta^{18}\text{O}$. While the spatiotemporal distribution of available instrumental observations is very limited, isotope-enabled models provide a perfectly observed, physically consistent framework to explore the interpretation of $\delta^{18}\text{O}_p$. Since iCAM5 is a state-of-the-art isotope-enabled model, which simulates the variability of $\delta^{18}\text{O}_p$ with high fidelity (Nusbaumer et al., 2017), and our previous result also shows that it successfully simulates the relationship between convective activity and $\delta^{18}\text{O}_p$, we now use it to diagnose the causes of $\delta^{18}\text{O}_p$ variability.

Here we estimate the contribution of stratiform fraction, OLR, precipitation amount, and local water vapor advection to the percentage of variance of $\delta^{18}\text{O}_p$ at monthly scales in iCAM5 by calculating the R^2 value between these variables. Water vapor advection is estimated by

$$\int_{p_s}^{p_{\text{top}}} -\mathbf{v} \cdot \nabla \delta^{18}\text{O}_v dp, \quad (1)$$

which is based on equation (4) derived in Okazaki et al. (2015), where p_s is surface pressure, p_{top} is pressure at the top of atmosphere, \mathbf{V} is wind, and $\delta^{18}\text{O}_v$ is water vapor $\delta^{18}\text{O}$. Since the advection term is calculated at each grid cell here, it only represents local water vapor advection and cannot describe the contribution of remote water vapor transport. Figure 8 shows the distribution of R^2 values over the Asian monsoon region. Since we are taking the interpretation of speleothem $\delta^{18}\text{O}$ as an example, many well-known Asian cave sites are also plotted on this map. These sites are included in the recent global compilation SISAL_v1 (Atsawawaranunt et al., 2018), produced by the PAGES (Past Global Changes, <http://www.pages-igbp.org/>) working group SISAL (Speleothem Isotopes Synthesis and AnaLysis, <http://www.pages-igbp.org/ini/wg/sisal/intro>).

Figure 8 shows that stratiform fraction contributes less than 10% of $\delta^{18}\text{O}_p$ variability in Chinese and Indian caves, while it contributes about 20% over the Maritime Continent (Borneo). OLR can explain as much as 50% over the Indochina Peninsula and 20% over the Maritime Continent (consistent with the observational result of Moerman et al., 2013, in Borneo) and still does not contribute more than 10% variability of $\delta^{18}\text{O}_p$ over China and India. The contribution of precipitation amount has a similar spatial distribution to OLR over land, showing that precipitation amount accounts for less than 10% of the variability of $\delta^{18}\text{O}_p$ in China and India (except the southeast corner of the Indian Peninsula), including the celebrated caves of Sanbao (Cheng et al., 2009, 2016) and Hulu (Cheng et al., 2006; Wang et al., 2001; Zhang et al., 2014). This result suggests that the contribution of convection is as important as precipitation amount over the Indochina Peninsula and the Maritime Continent, and neither convection nor precipitation amount explains much of the variability of precipitation over Chinese and Indian caves. This is in sharp contrast to the classic view that Chinese speleothem records represent local precipitation amount or the ratio of summer to winter precipitation (Cheng et al., 2009; Dykoski et al., 2005; Wang et al., 2001, 2008). Local water vapor advection generally contributes little to $\delta^{18}\text{O}_p$ (Figure 8d). The places where local water vapor advection contributes above 20% of $\delta^{18}\text{O}_p$ are scattered over central Asia and Northeast Asia. To estimate the total local contributions to $\delta^{18}\text{O}_p$, we perform multilinear regressions with these four factors and obtain the R^2 statistics. The result shows that local effects can explain much of variability of the $\delta^{18}\text{O}_p$ over the Indochina Peninsula, the Maritime Continent and caves north of 40°N (sum of $R^2 > 90\%$). However, local effects explain less than 20% of the variability of $\delta^{18}\text{O}_p$ over eastern China, northern India, and the Arabian Peninsula, where many caves exist. This suggests that over these locations, remote effects like the upstream effect raised by Pausata et al. (2011; e.g., Chinese speleothem $\delta^{18}\text{O}$ is influenced by precipitation over India) should contribute much to $\delta^{18}\text{O}_p$ variability. These contributions will be quantified in a follow-up study. It should be noted that this result is based on iCAM5, and iCAM5 simulates a smaller correlation of stratiform ratio and $\delta^{18}\text{O}_p$ compared with the observations, as shown in section 3.1. Also, these results are based on monthly data, so they mainly reflect seasonal/interannual variability of $\delta^{18}\text{O}_p$. Over millennia/orbital scales, there is strong coherence among speleothem $\delta^{18}\text{O}$ at different sites (Battisti et al., 2014; Cheng et al., 2012) even though $\delta^{18}\text{O}_p$ is controlled by many factors as we show here. This is partly because the climate signals over millennia/orbital scales usually feature relatively large amplitude and spatial scales. Another possible reason is $\delta^{18}\text{O}_p$ is more controlled by nonlocal processes, which represent more LS circulation features, if our results hold true for millennia/orbital scales. Tabor et al. (2018) employed ICESM/iCAM5 with the water-tagging technique to constrain the contribution of LS moisture source effects at orbital scales and found that the moisture source contributions are the dominant factor over the South Asian monsoon region.

4. Discussion and Conclusions

We evaluated the ability of seven isotope-enabled models to simulate the impact of convective activity on $\delta^{18}\text{O}_p$. The results show that only one (iCAM5) can simulate the negative correlation between stratiform fraction and $\delta^{18}\text{O}_p$ discovered in observations. The iCAM5 results are also consistent with Lacour et al. (2018) in that deeper convection corresponds to more negative $\delta^{18}\text{O}_p$. Models that do not simulate the anticorrelation between stratiform fraction and $\delta^{18}\text{O}_p$ may not be suitable to study the role of precipitation types on $\delta^{18}\text{O}_p$, but they can still be useful to investigate the role of other aspects of convection, such as convection depth, because all models investigated herein are found to simulate the observed relationship between OLR and $\delta^{18}\text{O}_p$. But we should also note that different models may have different mechanisms to generate this relationship—some getting the right answer for the wrong reasons.

Although iCAM5 successfully simulates the negative correlation between stratiform ratio and $\delta^{18}\text{O}_p$, it should be noted that iCAM5, like other models, largely underestimates stratiform fraction in the tropics (less than 10% while TRMM has over 40%; Figure 9). We also note that LMDZ simulates stratiform fraction fairly well in the tropics, even though it does not successfully reproduce the anticorrelation between stratiform rainfall fraction and $\delta^{18}\text{O}_p$. The underestimation of the stratiform ratio in the tropics in climate models is a common problem (Song & Yu, 2004), and some studies (Song & Zhang, 2011; Yang et al., 2013) proposed methods to improve its simulation, including modifying microphysics parameterization schemes. In addition, the resolution of GCMs is too coarse to represent organized convection and MCSs, and MCSs have high stratiform ratios, so adding a suitable and feasible parameterization of organized tropical convection for GCMs like that proposed by Moncrieff et al. (2017) may improve the simulation of stratiform fraction. Finally, we note that shallow convection precipitation in models like iCAM5 is categorized as convective precipitation though it accounts for a small (<5%) fraction of the total precipitation, but it shares some features (e.g., relatively stable atmospheric structure) with the defined stratiform precipitation in TRMM, and this may also underestimate the fraction of stratiform precipitation in models.

Lacour et al. (2018) argue that the relationship between stratiform fraction and $\delta^{18}\text{O}_p$ can be interpreted by the depth of convection instead of cloud microphysics processes mentioned in Aggarwal et al. (2016), because stratiform convection has a higher condensation level, which corresponds to low $\delta^{18}\text{O}_p$. Our results partially reconcile these arguments, in that cloud microphysics at least can explain low $\delta^{18}\text{O}$ in stratiform precipitation because more ice particles form at high altitude with low temperature in stratiform precipitation, resulting in low raindrop $\delta^{18}\text{O}$ (Figure 5b). This is one plausible reason that deep convection may be associated with depleted $\delta^{18}\text{O}_p$, apart from downdrafts and reevaporation described in Lacour et al. (2018). Shallow convection also occurs in iCAM5, and it is unclear if the explanation of Aggarwal et al. (2016) for convective precipitation applies for both deep and shallow convection.

Lastly, we investigated the quantitative contribution of convective activity to $\delta^{18}\text{O}_p$ variability in the Asian monsoon region in iCAM5. The result shows that the role of convection is very important in the Indochina Peninsula, where the variation of OLR is associated with as much as 50% of the variance of $\delta^{18}\text{O}_p$, and OLR is an indicator of LS convective activity and convection depth. This suggests that paleoclimate records there can be partly interpreted as the variability of LS convection, which can be connected to intraseasonal variability like the Madden-Julian Oscillation. However, the result shows that neither convection nor precipitation amount can explain more than 15% of $\delta^{18}\text{O}_p$ over China and India. This result is in stark contrast to the traditional interpretation of Chinese speleothem $\delta^{18}\text{O}$, taken to represent local precipitation amount or the ratio of summer to winter precipitation. If so, this suggests a dominant influence of remote water vapor transport, including the origin of water vapor source (circulation variation), fractionation in water vapor along the transport path, and fractionation at the water vapor source (e.g., SST effect, Pausata et al., 2011)—a hypothesis that we will investigate in a follow-up study. This analysis is based on monthly mean data, which largely reflects the seasonal variability, and recent studies (Eastoe & Dettman, 2016) show that seasonal relationships between $\delta^{18}\text{O}_p$ and climate variables may not hold true for longer time scales. Whether local contributions to the variability of $\delta^{18}\text{O}_p$ are still small for interannual-decadal or longer time scales deserves careful investigation. We should note that this result is based on one model, and validation by observations is also necessary.

Compared with previous isotope-enabled model evaluations (Conroy et al., 2013; Midhun & Ramesh, 2016; Risi et al., 2012), we mainly focused on the role of convective activity and tried to quantify the contribution of precipitation amount, convection, and local water vapor advection. Our results, like these previous studies, show a large model spread in simulating relationships between water isotopes and climate variables, indicating the unique ability of water isotope observations to discriminate between models.

Our results suggest that a state-of-art model like iCAM5 can successfully simulate the role of convection in the variability of $\delta^{18}\text{O}_p$, which gives us confidence in using this model to study the interpretation of $\delta^{18}\text{O}_p$ and hydrological paleoclimate records. It also implies that there are no shortcuts for isotope-enabled models to simulate the role of precipitation types in $\delta^{18}\text{O}_p$. The necessary processes in cloud microphysics have to be captured if we want to use models to study the impact of convection on $\delta^{18}\text{O}_p$. Also, isotope-enabled models, which provide water isotope ratios that standard GCMs do not track, can be used to constrain convective and microphysical processes in GCMs, which should help improve future climate projections.

Acknowledgments

We thank Pradeep Aggarwal for helpful discussions. This work was supported by a Dornsife Merit Fellowship from the University of Southern California (USC). We thank Sarah Feakins and Naomi M. Levine for initiating this investigation. SWING2 model data are available at <https://data.giss.nasa.gov/swing2/>. SPEEDY-IER and ICAM5 data are at <https://doi.org/10.5281/zenodo.1438547>.

References

- Aggarwal, P. K., Romatschke, U., Araguas-Araguas, L., Belachew, D., Longstaffe, F. J., Berg, P., et al. (2016). Proportions of convective and stratiform precipitation revealed in water isotope ratios. *Nature Geoscience*, 9(8), 624. <https://doi.org/10.1038/ngeo2739>
- Arakawa, A., & Schubert, W. H. (1974). Interaction of a cumulus cloud ensemble with the large-scale environment, part i. *Journal of the Atmospheric Sciences*, 31(3), 674–701.
- Atsawaranunt, K., Comas-Bru, L., Amirnezhad Mozhdehi, S., Deininger, M., Harrison, S. P., Baker, A., et al. (2018). The SISAL database: A global resource to document oxygen and carbon isotope records from speleothems. *Earth System Science Data*, 10, 1687–1713. <https://doi.org/10.5194/essd-10-1687-2018>
- Baker, A., Bradley, C., Phipps, S., Fischer, M., Fairchild, I., Fuller, L., et al. (2012). Millennial-length forward models and pseudoproxies of stalagmite $\delta^{18}\text{O}$: an example from NW Scotland. *Climate of the Past*, 8(4), 1153–1167. <https://doi.org/10.5194/cp-8-1153-2012>
- Battisti, D., Ding, Q., & Roe, G. (2014). Coherent pan-Asian climatic and isotopic response to orbital forcing of tropical insolation. *Journal of Geophysical Research: Atmospheres*, 119, 11–997. <https://doi.org/10.1002/2014JD021960>
- Benjamini, Y., & Hochberg, Y. (1995). Controlling the false discovery rate: A practical and powerful approach to multiple testing. *Journal of the Royal Statistical Society. Series B (Methodological)*, 57, 289–300.
- Bony, S., Risi, C., & Vimeux, F. (2008). Influence of convective processes on the isotopic composition ($\delta^{18}\text{O}$ and δD) of precipitation and water vapor in the tropics: 1. Radiative-convective equilibrium and Tropical Ocean–Global Atmosphere–Coupled Ocean-Atmosphere Response Experiment (TOGA-COARE) simulations. *Journal of Geophysical Research*, 113, D19305. <https://doi.org/10.1029/2008JD009942>
- Cai, Z., & Tian, L. (2016). Atmospheric controls on seasonal and interannual variations in the precipitation isotope in the East Asian monsoon region. *Journal of Climate*, 29(4), 1339–1352. <https://doi.org/10.1175/JCLI-D-15-0363.1>
- Cheng, H., Edwards, R. L., Broecker, W. S., Denton, G. H., Kong, X., Wang, Y., et al. (2009). Ice age terminations. *Science*, 326(5950), 248–252. <https://doi.org/10.1126/science.1177840>
- Cheng, H., Edwards, R. L., Sinha, A., Spötl, C., Yi, L., Chen, S., et al. (2016). The Asian monsoon over the past 640,000 years and ice age terminations. *Nature*, 534(7609), 640–646. <https://doi.org/10.1038/nature18591>
- Cheng, H., Edwards, R. L., Wang, Y., Kong, X., Ming, Y., Kelly, M. J., et al. (2006). A penultimate glacial monsoon record from Hulu Cave and two-phase glacial terminations. *Geology*, 34(3), 217–220. <https://doi.org/10.1130/G22289.1>
- Cheng, H., Sinha, A., Wang, X., Cruz, F. W., & Edwards, R. L. (2012). The global paleomonsoon as seen through speleothem records from Asia and the Americas. *Climate Dynamics*, 39(5), 1045–1062.
- Conroy, J. L., Cobb, K. M., & Noone, D. (2013). Comparison of precipitation isotope variability across the tropical Pacific in observations and SWING2 model simulations. *Journal of Geophysical Research: Atmospheres*, 118, 5867–5892. <https://doi.org/10.1002/jgrd.50412>
- Dai, A. (2006). Precipitation characteristics in eighteen coupled climate models. *Journal of Climate*, 19(18), 4605–4630. <https://doi.org/10.1175/JCLI3884.1>
- Dansgaard, W. (1964). Stable isotopes in precipitation. *Tellus*, 16(4), 436–468. <https://doi.org/10.1111/j.2153-3490.1964.tb00181.x>
- Dee, S., Emile-Geay, J., Evans, M. N., Allam, A., Steig, E. J., & Thompson, D. M. (2015). PRYSM: An open-source framework for PRoxy System Modeling, with applications to oxygen-isotope systems. *Journal of Advances in Modeling Earth Systems*, 7, 1220–1247. <https://doi.org/10.1002/2015MS000447>
- Dee, S., Noone, D., Buennings, N., Emile-Geay, J., & Zhou, Y. (2015). SPEEDY-IER: A fast atmospheric GCM with water isotope physics. *Journal of Geophysical Research: Atmospheres*, 120, 73–91. <https://doi.org/10.1002/2014JD022194>
- Dee, S. G., Parsons, L. A., Loope, G. R., Overpeck, J. T., Ault, T. R., & Emile-Geay, J. (2017). Improved spectral comparisons of paleoclimate models and observations via proxy system modeling: Implications for multi-decadal variability. *Earth and Planetary Science Letters*, 476(Supplement C), 34–46. <https://doi.org/10.1016/j.epsl.2017.07.036>
- Dykoski, C. A., Edwards, R. L., Cheng, H., Yuan, D., Cai, Y., Zhang, M., et al. (2005). A high-resolution, absolute-dated Holocene and deglacial Asian monsoon record from Dongge Cave, China. *Earth and Planetary Science Letters*, 233(1), 71–86. <https://doi.org/10.1016/j.epsl.2005.01.036>
- Eastoe, C., & Dettman, D. (2016). Isotope amount effects in hydrologic and climate reconstructions of monsoon climates: Implications of some long-term data sets for precipitation. *Chemical Geology*, 430, 78–89.
- Ebisuzaki, W. (1997). A method to estimate the statistical significance of a correlation when the data are serially correlated. *Journal of Climate*, 10(9), 2147–2153. [https://doi.org/10.1175/1520-0442\(1997\)010<2147:AMTETS>2.0.CO;2](https://doi.org/10.1175/1520-0442(1997)010<2147:AMTETS>2.0.CO;2)
- Emanuel, K. A., & Živković-Rothman, M. (1999). Development and evaluation of a convection scheme for use in climate models. *Journal of the Atmospheric Sciences*, 56(11), 1766–1782.
- Emile-Geay, J., & Tingley, M. (2016). Inferring climate variability from nonlinear proxies: Application to palaeo-ENSO studies. *Climate of the Past*, 12(1), 31–50.
- Evans, M. N., Tolwinski-Ward, S. E., Thompson, D. M., & Anchukaitis, K. J. (2013). Applications of proxy system modeling in high resolution paleoclimatology. *Quaternary Science Reviews*, 76(0), 16–28. <https://doi.org/10.1016/j.quascirev.2013.05.024>
- Field, R. D., Kim, D., LeGrande, A. N., Worden, J., Kelley, M., & Schmidt, G. A. (2014). Evaluating climate model performance in the tropics with retrievals of water isotopic composition from Aura TES. *Geophysical Research Letters*, 41, 6030–6036. <https://doi.org/10.1002/2014GL060572>
- Frappier, A. B., Sahagian, D., Carpenter, S. J., González, L. A., & Frappier, B. R. (2007). Stalagmite stable isotope record of recent tropical cyclone events. *Geology*, 35(2), 111–114. <https://doi.org/10.1130/G23145A.1>
- Funk, A., Schumacher, C., & Awaka, J. (2013). Analysis of rain classifications over the tropics by version 7 of the TRMM PR 2A23 algorithm. *Journal of the Meteorological Society of Japan. Ser. II*, 91(3), 257–272. <https://doi.org/10.2151/jmsj.2013-302>
- Galewsky, J., Steen-Larsen, H. C., Field, R. D., Worden, J., Risi, C., & Schneider, M. (2016). Stable isotopes in atmospheric water vapor and applications to the hydrologic cycle. *Reviews of Geophysics*, 54, 809–865. <https://doi.org/10.1002/2015RG000512>
- Gregory, D., & Rowntree, P. (1990). A mass flux convection scheme with representation of cloud ensemble characteristics and stability-dependent closure. *Monthly Weather Review*, 118(7), 1483–1506.
- Hoffmann, G., Werner, M., & Heimann, M. (1998). Water isotope module of the ECHAM atmospheric general circulation model: A study on timescales from days to several years. *Journal of Geophysical Research*, 103(D14), 16,871–16,896. <https://doi.org/10.1029/98JD00423>
- Houze, R. A. (1997). Stratiform precipitation in regions of convection: A meteorological paradox? *Bulletin of the American Meteorological Society*, 78(10), 2179–2196. [https://doi.org/10.1175/1520-0477\(1997\)078<2179:SPIROC>2.0.CO;2](https://doi.org/10.1175/1520-0477(1997)078<2179:SPIROC>2.0.CO;2)
- Hu, J., Emile-Geay, J., & Partin, J. (2017). Correlation-based interpretations of paleoclimate data—Where statistics meet past climates. *Earth and Planetary Science Letters*, 459, 362–371. <https://doi.org/10.1016/j.epsl.2016.11.048>
- Hurrell, J. W., Hack, J. J., Shea, D., Caron, J. M., & Rosinski, J. (2008). A new sea surface temperature and sea ice boundary dataset for the community atmosphere model. *Journal of Climate*, 21(19), 5145–5153.

- Jex, C., Phipps, S., Baker, A., & Bradley, C. (2013). Reducing uncertainty in the climatic interpretations of speleothem $\delta^{18}\text{O}$. *Geophysical Research Letters*, 40, 2259–2264. <https://doi.org/10.1002/grl.50467>
- Joussaume, S., Sadourny, R., & Jouzel, J. (1984). A general circulation model of water isotope cycles in the atmosphere. *Nature*, 311(5981), 24. <https://doi.org/10.1038/311024a0>
- Jouzel, J., Russell, G., Suozzo, R., Koster, R., White, J., & Broecker, W. (1987). Simulations of the HDO and H_2^{18}O atmospheric cycles using the NASA GISS general circulation model: The seasonal cycle for present-day conditions. *Journal of Geophysical Research*, 92(D12), 14,739–14,760. <https://doi.org/10.1029/JD092D12p14739>
- Kurita, N. (2013). Water isotopic variability in response to mesoscale convective system over the tropical ocean. *Journal of Geophysical Research: Atmospheres*, 118, 10,376–10,390. <https://doi.org/10.1029/jgrd.50754>
- Kurita, N., Noone, D., Risi, C., Schmidt, G. A., Yamada, H., & Yoneyama, K. (2011). Intraseasonal isotopic variation associated with the Madden-Julian Oscillation. *Journal of Geophysical Research*, 116, D24101. <https://doi.org/10.1029/2010JD015209>
- Lacour, J.-L., Risi, C., Worden, J., Clerbaux, C., & Coheur, P.-F. (2018). Importance of depth and intensity of convection on the isotopic composition of water vapor as seen from IASI and TES δD observations. *Earth and Planetary Science Letters*, 481, 387–394. <https://doi.org/10.1016/j.epsl.2017.10.048>
- Lawrence, J. R., Gedzelman, S. D., Dexheimer, D., Cho, H.-K., Carrie, G. D., Gasparini, R., et al. (2004). Stable isotopic composition of water vapor in the tropics. *Journal of Geophysical Research*, 109, D06115. <https://doi.org/10.1029/2003JD004046>
- Lee, J.-E., & Fung, I. (2008). "Amount effect" of water isotopes and quantitative analysis of post-condensation processes. *Hydrological Processes*, 22(1), 1–8. <https://doi.org/10.1002/hyp.6637>
- Lee, J.-E., Fung, I., DePaolo, D. J., & Henning, C. C. (2007). Analysis of the global distribution of water isotopes using the NCAR atmospheric general circulation model. *Journal of Geophysical Research*, 112, D16306. <https://doi.org/10.1029/2006JD007657>
- Lee, J.-E., Pierrehumbert, R., Swann, A., & Lintner, B. R. (2009). Sensitivity of stable water isotopic values to convective parameterization schemes. *Geophysical Research Letters*, 36, L23801. <https://doi.org/10.1029/2009GL040880>
- Lekshmy, P., Midhun, M., Ramesh, R., & Jani, R. (2014). ^{18}O depletion in monsoon rain relates to large scale organized convection rather than the amount of rainfall. *Scientific Reports*, 4, 5661. <https://doi.org/10.1038/srep05661>
- Liebmann, B. (1996). Description of a complete (interpolated) outgoing longwave radiation dataset. *Bulletin of the American Meteorological Society*, 77, 1275–1277.
- Maher, B. A., & Thompson, R. (2012). Oxygen isotopes from Chinese caves: Records not of monsoon rainfall but of circulation regime. *Journal of Quaternary Science*, 27(6), 615–624. <https://doi.org/10.1002/jqs.2553>
- Midhun, M., & Ramesh, R. (2016). Validation of ^{18}O as a proxy for past monsoon rain by multi-GCM simulations. *Climate Dynamics*, 46(5–6), 1371–1385. <https://doi.org/10.1007/s00382-015-2652-8>
- Moerman, J. W., Cobb, K. M., Adkins, J. F., Sodemann, H., Clark, B., & Tuen, A. A. (2013). Diurnal to interannual rainfall $\delta^{18}\text{O}$ variations in northern Borneo driven by regional hydrology. *Earth and Planetary Science Letters*, 369, 108–119. <https://doi.org/10.1016/j.epsl.2013.03.014>
- Moncrieff, M. W., Liu, C., & Bogenschutz, P. (2017). Simulation, modeling, and dynamically based parameterization of organized tropical convection for global climate models. *Journal of the Atmospheric Sciences*, 74(5), 1363–1380. <https://doi.org/10.1175/JAS-D-16-0166.1>
- Moorthi, S., & Suarez, M. J. (1992). Relaxed Arakawa-Schubert: A parameterization of moist convection for general circulation models. *Monthly Weather Review*, 120(6), 978–1002.
- Nesbitt, S. W., Cifelli, R., & Rutledge, S. A. (2006). Storm morphology and rainfall characteristics of TRMM precipitation features. *Monthly Weather Review*, 134(10), 2702–2721. <https://doi.org/10.1175/MWR3200.1>
- Noone, D., & Simmonds, I. (2002). Associations between $\delta^{18}\text{O}$ of water and climate parameters in a simulation of atmospheric circulation for 1979–95. *Journal of Climate*, 15(22), 3150–3169. [https://doi.org/10.1175/1520-0442\(2002\)015<3150:ABOOWA>2.0.CO;2](https://doi.org/10.1175/1520-0442(2002)015<3150:ABOOWA>2.0.CO;2)
- Nusbaumer, J., Wong, T. E., Bardeen, C., & Noone, D. (2017). Evaluating hydrological processes in the Community Atmosphere Model Version 5 (CAM5) using stable isotope ratios of water. *Journal of Advances in Modeling Earth Systems*, 9, 949–977. <https://doi.org/10.1029/2016MS000839>
- Okazaki, A., Satoh, Y., Tremoy, G., Vimeux, F., Scheepmaker, R., & Yoshimura, K. (2015). Interannual variability of isotopic composition in water vapor over western Africa and its relationship to ENSO. *Atmospheric Chemistry and Physics*, 15(6), 3193–3204. <https://doi.org/10.5194/acp-15-3193-2015>
- Park, S., & Bretherton, C. S. (2009). The University of Washington shallow convection and moist turbulence schemes and their impact on climate simulations with the community atmosphere model. *Journal of Climate*, 22(12), 3449–3469.
- Pausata, F. S., Battisti, D. S., Nisancioğlu, K. H., & Bitz, C. M. (2011). Chinese stalagmite ^{18}O controlled by changes in the Indian monsoon during a simulated Heinrich event. *Nature Geoscience*, 4(7), 474–480. <https://doi.org/10.1038/ngeo1169>
- Risi, C., Bony, S., & Vimeux, F. (2008). Influence of convective processes on the isotopic composition ($\delta^{18}\text{O}$ and δD) of precipitation and water vapor in the tropics: 2. Physical interpretation of the amount effect. *Journal of Geophysical Research*, 113, D19306. <https://doi.org/10.1029/2008JD009943>
- Risi, C., Bony, S., Vimeux, F., & Jouzel, J. (2010). Water-stable isotopes in the LMDZ4 general circulation model: Model evaluation for present-day and past climates and applications to climatic interpretations of tropical isotopic records. *Journal of Geophysical Research*, 115, D12118. <https://doi.org/10.1029/2009JD013255>
- Risi, C., Noone, D., Worden, J., Frankenberg, C., Stiller, G., Kiefer, M., et al. (2012). Process-evaluation of tropospheric humidity simulated by general circulation models using water vapor isotopologues: 1. Comparison between models and observations. *Journal of Geophysical Research*, 117, D05303. <https://doi.org/10.1029/2011JD016621>
- Schmidt, G. A., LeGrande, A. N., & Hoffmann, G. (2007). Water isotope expressions of intrinsic and forced variability in a coupled ocean-atmosphere model. *Journal of Geophysical Research*, 112, D10103. <https://doi.org/10.1029/2006JD007781>
- Sinha, A., Berkelhammer, M., Stott, L., Mudelsee, M., Cheng, H., & Biswas, J. (2011). The leading mode of Indian summer monsoon precipitation variability during the last millennium. *Geophysical Research Letters*, 38, L15703. <https://doi.org/10.1029/2011GL047713>
- Song, X., & Yu, R. (2004). Underestimated tropical stratiform precipitation in the National Center for Atmospheric Research (NCAR) Community Climate Model (CCM3). *Geophysical Research Letters*, 31, L24101. <https://doi.org/10.1029/2004GL021292>
- Song, X., & Zhang, G. J. (2011). Microphysics parameterization for convective clouds in a global climate model: Description and single-column model tests. *Journal of Geophysical Research*, 116, D02201. <https://doi.org/10.1029/2010JD014833>
- Tabor, C. R., Otto-Bliesner, B. L., Brady, E. C., Nusbaumer, J., Zhu, J., Erb, M. P., et al. (2018). Interpreting precession-driven ^{18}O variability in the South Asian monsoon region. *Journal of Geophysical Research: Atmospheres*, 123, 5927–5946. <https://doi.org/10.1029/2018JD028424>
- Tan, M. (2014). Circulation effect: Response of precipitation ^{18}O to the ENSO cycle in monsoon regions of China. *Climate Dynamics*, 42(3–4), 1067–1077. <https://doi.org/10.1007/s00382-013-1732-x>

- Tharammal, T., Bala, G., & Noone, D. (2017). Impact of deep convection on the isotopic amount effect in tropical precipitation. *Journal of Geophysical Research: Atmospheres*, 122, 1505–1523. <https://doi.org/10.1002/2016JD025555>
- Tian, L., Yao, T., MacClune, K., White, J., Schilla, A., Vaughn, B., et al. (2007). Stable isotopic variations in west China: A consideration of moisture sources. *Journal of Geophysical Research*, 112, D10112. <https://doi.org/10.1029/2006JD007718>
- Tiedtke, M. (1989). A comprehensive mass flux scheme for cumulus parameterization in large-scale models. *Monthly Weather Review*, 117(8), 1779–1800.
- Tindall, J., Valdes, P., & Sime, L. C. (2009). Stable water isotopes in HadCM3: Isotopic signature of El Niño–Southern Oscillation and the tropical amount effect. *Journal of Geophysical Research*, 114, D04111. <https://doi.org/10.1029/2008JD010825>
- Wang, Y.-J., Cheng, H., Edwards, R. L., An, Z., Wu, J., Shen, C.-C., & Dorale, J. A. (2001). A high-resolution absolute-dated late Pleistocene monsoon record from Hulu Cave, China. *Science*, 294(5550), 2345–2348. <https://doi.org/10.1126/science.1064618>
- Wang, Y., Cheng, H., Edwards, R. L., Kong, X., Shao, X., Chen, S., et al. (2008). Millennial-and orbital-scale changes in the East Asian monsoon over the past 224,000 years. *Nature*, 451(7182), 1090–1093. <https://doi.org/10.1038/nature06692>
- Yadava, M., Ramesh, R., & Pant, G. (2004). Past monsoon rainfall variations in peninsular India recorded in a 331-year-old speleothem. *The Holocene*, 14(4), 517–524. <https://doi.org/10.1191/0959683604hl728rp>
- Yang, B., Qian, Y., Lin, G., Leung, L. R., Rasch, P. J., Zhang, G. J., et al. (2013). Uncertainty quantification and parameter tuning in the CAM5 Zhang-McFarlane convection scheme and impact of improved convection on the global circulation and climate. *Journal of Geophysical Research: Atmospheres*, 118, 395–415. <https://doi.org/10.1029/2012JD018213>
- Yoshimura, K., Kanamitsu, M., Noone, D., & Oki, T. (2008). Historical isotope simulation using reanalysis atmospheric data. *Journal of Geophysical Research*, 113, D19108. <https://doi.org/10.1029/2008JD010074>
- Yuan, D., Cheng, H., Edwards, R. L., Dykoski, C. A., Kelly, M. J., Zhang, M., et al. (2004). Timing, duration, and transitions of the last interglacial Asian monsoon. *Science*, 304(5670), 575–578. <https://doi.org/10.1126/science.1091220>
- Zhang, G. J., & McFarlane, N. A. (1995). Sensitivity of climate simulations to the parameterization of cumulus convection in the Canadian climate centre general circulation model. *Atmosphere-ocean*, 33(3), 407–446.
- Zhang, W., Wu, J., Wang, Y., Wang, Y., Cheng, H., Kong, X., & Duan, F. (2014). A detailed East Asian monsoon history surrounding the ‘Mystery Interval’ derived from three Chinese speleothem records. *Quaternary Research*, 82(1), 154–163. <https://doi.org/10.1016/j.yqres.2014.01.010>